Impact-Toughening Mechanisms of Calcium Carbonate-Reinforced Polypropylene Nanocomposite

J.-I. Weon,[1] K.-T. Gam,[1] W.-J. Boo,[1] H.-J. Sue,[1] C.-M. Chan[2]

[1]*Polymer Technology Center, Department of Mechanical Engineering, Texas A&M University, College Station, Texas 77843–312*
[2]*Department of Chemical Engineering, The Hong Kong University of Science and Technology, Clear Water Bay, Hong Kong*

Received 29 December 2005; accepted 18 May 2005
DOI 10.1002/app.22909
Published online in Wiley InterScience (www.interscience.wiley.com).

ABSTRACT: The impact fracture mechanisms of polypropylene (PP), containing 9.2 vol % of calcium carbonate ($CaCO_3$) nanoparticles, were investigated using optical microscopy and transmission electron microscopy. The incorporation of $CaCO_3$ nanoparticles reduces the size of spherulites and induces the formation of β-phase crystallites, which leads to a more ductile PP matrix. Double-notch four-point bending (DN-4PB) Charpy impact specimens and notched Izod impact specimens were utilized to study the fracture mechanism(s) responsible for the observed toughening effect. A detailed investigation reveals that the $CaCO_3$ nanoparticles act as stress concentrators to initiate massive crazes, followed by shear banding in PP matrix. These toughening mechanisms are responsible for the observed, improved impact strength. A comparison of the fracture mechanisms observed between DN-4PB Charpy and Izod impact tests is also made to show the effectiveness of DN-4PB for investigation of impact fracture mechanisms of polymeric systems. © 2006 Wiley Periodicals, Inc. J Appl Polym Sci 99: 3070–3076, 2006

Key words: calcium carbonate; PP nanocomposite; impact strength; crazing; shear yielding

INTRODUCTION

It is well known that inorganic fillers are effective in improving stiffness, hardness, chemical resistance, and dimension stability, as well as gas-barrier properties of polymers.[1–10] Considerable literature can be found, with focuses on improving the mechanical properties of polypropylene (PP) using various kinds of fillers.[8–10] The effectiveness of inorganic fillers on improving physical and mechanical properties of PP strongly depends on the filler size, shape, aspect ratio, interfacial adhesion, surface characteristics, and degree of dispersion.[11–13]

Calcium carbonate ($CaCO_3$) particles have a nearly isotropic particulate structure.[14] The addition of such an inorganic rigid filler to a semicrystalline polymer matrix may affect crystal structure, crystallinity, spherulite size, lamellar thickness, and thickness of interlamella amorphous layers. Typically, inorganic particle-filled polymer composites show an increase in modulus, but a decrease in toughness and ductility, mainly because of the induced stress concentration, agglomeration, and confinement of matrix molecular mobility around the rigid filler phase. However, a few exceptions have also been reported in the literature. In toughening polyethylene, $CaCO_3$ and chalk particles have been shown to be able to improve toughness of PE effectively.[15–17] For PP, Thio and coworkers[18] found that the $CaCO_3$-toughened PP composites could exhibit greatly improved impact strengths up to 40–50 kJ/m^2, as compared to 2–8 kJ/m^2 for that of neat PP. More recently, Chan et al.[14] showed that the fracture toughness of PP could be enhanced by over 300% by incorporating nanometer-sized (~40 nm) $CaCO_3$ particles.

In this study, investigation will be focused on understanding the underlying toughening mechanisms responsible for the impressive toughening effect found in PP/$CaCO_3$ nanocomposite. Roles of $CaCO_3$ nanoparticles on PP crystalline size, crystalline structure, and the observed toughening effect are also studied and discussed.

EXPERIMENTAL

Materials

PP homopolymer, PD403 (density, 1.04 g/cc) from Basell, USA, was used in this study. $CaCO_3$ nanopar-

Correspondence to: H.-J. Sue (hjsue@tamu.edu).
Contract grant sponsor: Defense Logistic Agency; contract grant number: SP0103–02-D-0024.
Contract grant sponsor: ARP Grant (The State of Texas); contract grant numbers: 000512–00137–2001.
Contract grant sponsor: The Hong Kong Government Research Grants Council; contract grant number: HKUST 6043/01P.
Contract grant sponsor: The Hong Kong University of Science and Technology; contract grant number: HIA 03/04.EG02.

TABLE I
Chemical Composition (wt %) of the $CaCO_3$ Nanoparticles

	Chemical composition (wt %)
C	12.9
O	44.2
H	0.5
Ca	41.6
Mg	0.6
Al	0.2

ticles were obtained from Guang Ping Nano Technology Group Ltd. The average primary particle size of $CaCO_3$ is about 44 nm. Irganox 1010® (Ciba Specialty Chemicals, Tarrytown, NY) was used as an antioxidant. The chemical composition of $CaCO_3$ nanoparticles was measured by inductively coupled plasma spectroscopy (Perkin–Elmer Optima 3000 ICP), and the content of carbon and hydrogen was determined by a carbon, hydrogen, and nitrogen analyzer (Table I). The $CaCO_3$ nanoparticles used in this study were surface-modified by stearic acid.

Sample preparation

Prior to mixing, PP and $CaCO_3$ were dried in an oven at 120°C for an hour, and then cooled to room temperature and kept in a desiccator. Compounding was carried out at 180°C, with a rotor speed of 60 rpm in a batch mixer (Haake 40 System). The content of $CaCO_3$ nanoparticles in PP matrix was 9.2 vol %.

The samples used in this study were injection-molded. For comparison, neat PP sample was also prepared. The detailed description of the sample preparation has been documented using injection-molding process.[14] Izod impact bars, with dimensions of 64 $\times$ 12.7 $\times$ 3.2 mm^3, were notched with a notch cutter (250-μm tip radius) to a notch depth of 3 mm, in accordance to ASTM D 256. The double notch four-point bending (DN-4PB) specimens were first notched with a 250-μm radius notch cutter to a depth of 3 mm, followed by tapping two nearly identical sharp cracks

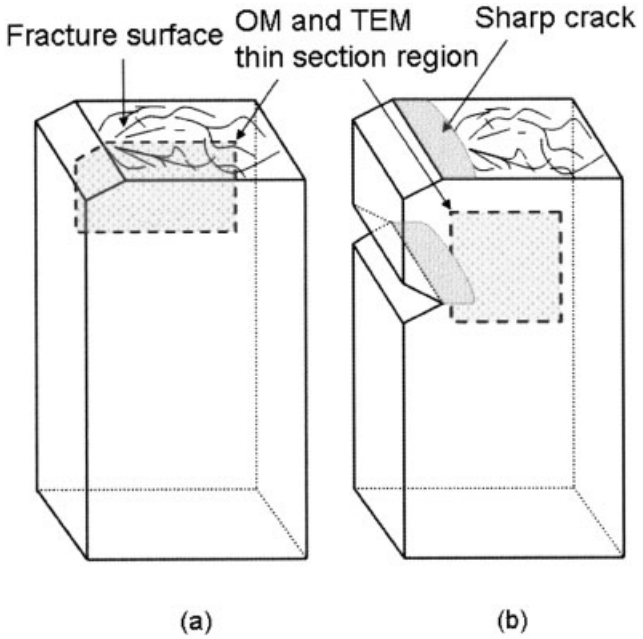

Figure 1 Schematic of the impact specimens used for OM and TEM observation: (a) notched Izod impact specimen and (b) DN-4PB Charpy impact specimen.

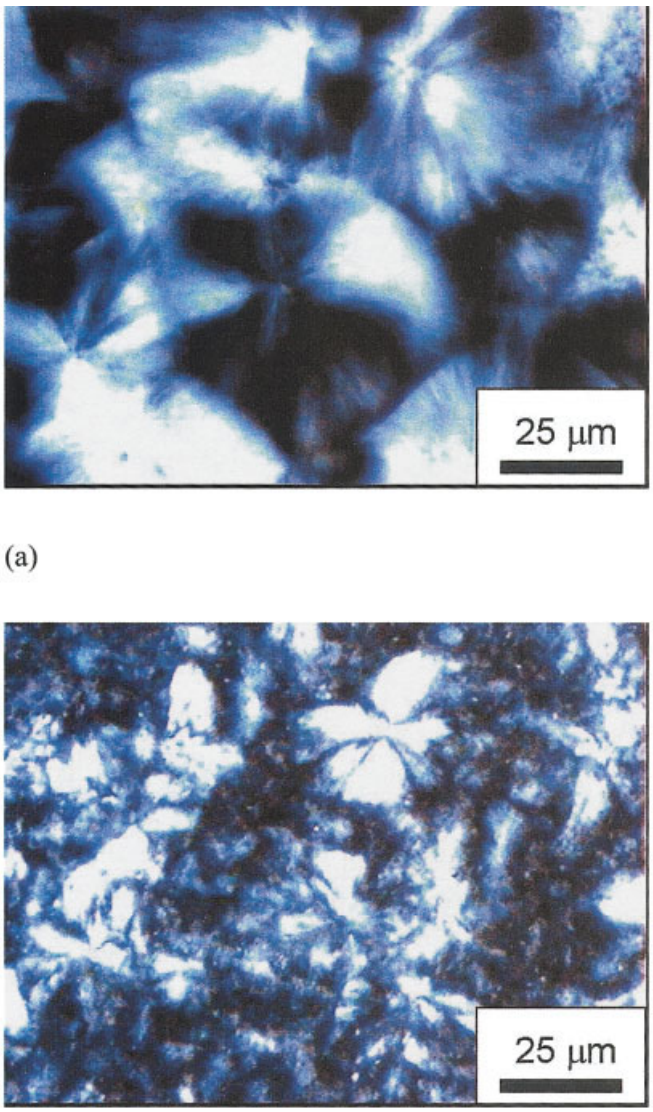

Figure 2 TOM under cross polarized field: (a) neat PP and (b) PP/$CaCO_3$ nanocomposite. [Color figure can be viewed in the online issue, which is available at www.interscience.wiley.com.]

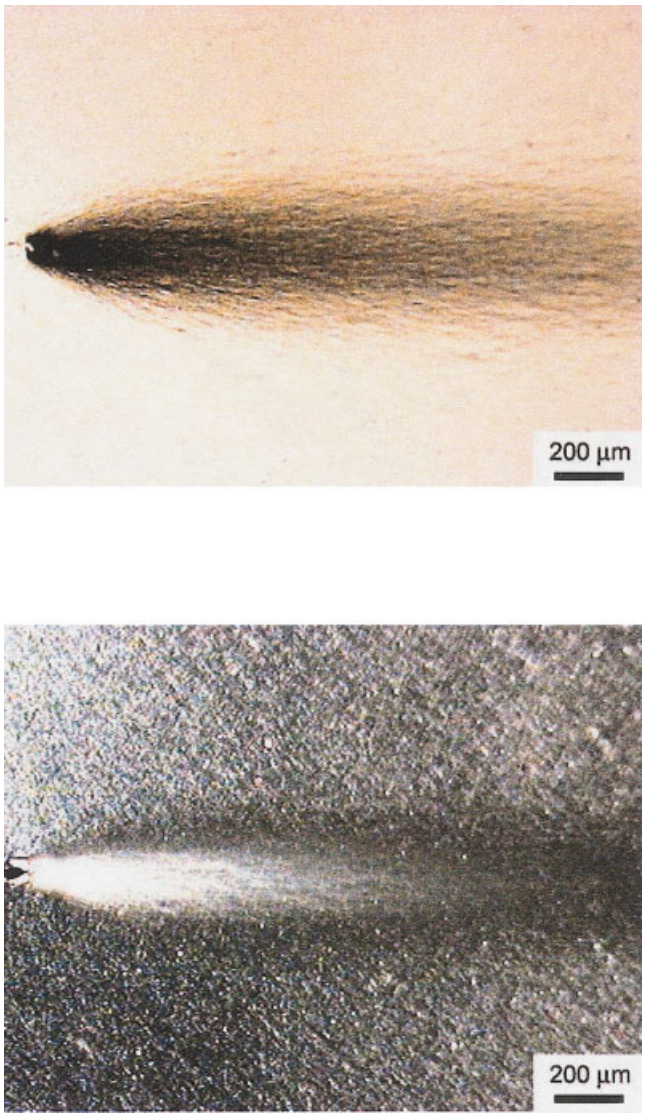

Figure 3 TOM of DN-4PB Charpy impact damage zone of PP/$CaCO_3$ nanocomposite: (a) bright field and (b) cross polarized field. The crack propagates from left to right. [Color figure can be viewed in the online issue, which is available at www.interscience.wiley.com.]

ahead of the two notches, using a liquid nitrogen-chilled razor blade. Notched Izod impact test and DN-4PB Charpy impact test were conducted at room temperature on a pendulum impact tester (Model TMI-43–02) with a single-head striker and a double-head striker, respectively.

Microscopy and toughening mechanism investigation

Optical microscopy (OM) and transmission electron microscopy (TEM) were employed to observe the morphology and to determine the fracture mechanisms of the nanocomposite specimens, after the impact tests. The impact damage zones were cut along the crack propagation direction, but perpendicular to the plane of fracture surface, using a diamond saw. The plane-strain core regions of the damage zone were prepared for OM and TEM observations (Fig. 1). For OM investigations, the damage zones of the impact specimens were polished into thin sections, with thicknesses of about 40–80 μm, following the procedures described by Holik et al.[19] These thin sections were investigated using an Olympus BX60 OM, under both bright field and cross polarization conditions, to observe the overall damage zone and features.

For the TEM effort (JEOL JEM1200EX), the plane-strain region of the damage zone was isolated and embedded in an epoxy mount and cured at room temperature, to avoid thermally induced stress on the sample. The cured epoxy bock was carefully trimmed to a size of 0.3×0.3 mm^2, and then faced-off using a diamond knife prior to staining. The face-off block were then stained with ruthenium tetra oxide (RuO_4) and cut into thin sections, using a Richard Chung Ultracut® microtome. Staining with RuO_4 was necessary, to allow for better image contrast between $CaCO_3$ particles and the PP matrix. The staining of RuO_4 also helped to harden the PP matrix and fill in the voids inside the craze bands, which stabilize the integrity of craze structure during microtoming. In this study, thin sections of about 90 nm in thickness were prepared and placed on 100-mesh Formvar/carbon-coated copper grids, for TEM observation.

RESULTS AND DISCUSSION

The incorporation of $CaCO_3$ nanoparticles in PP matrix can greatly affect the morphology of the PP matrix, which may influence the ductility and toughenability of PP. As shown in Figure 2, the sizes of spherulites (<30 μm) found in the PP/$CaCO_3$ nanocomposite are much smaller than those found in neat PP (>50 μm). This suggests that $CaCO_3$ nanoparticles are effective nucleating agents for PP.[14] A decrease in spherulite size should positively contribute to the toughenability of semicrystalline polymers.[20,21] In a previous work by Chan et al.,[14] the differential scanning calorimetry results indicated the presence of a small amount of β-phase PP, after the addition of $CaCO_3$ nanoparticles. Labour et al.[22] found that, since the β-phase has less crystal density than that of the α phase, the β-phase PP exhibits a lower modulus by about 10% and a reduced hardness by 15%, respectively, than the α-phase PP. The presence of the β-phase crystal around the $CaCO_3$ particles in PP may greatly affect the operative toughening mechanisms in the PP/$CaCO_3$ nanocomposite, as well.

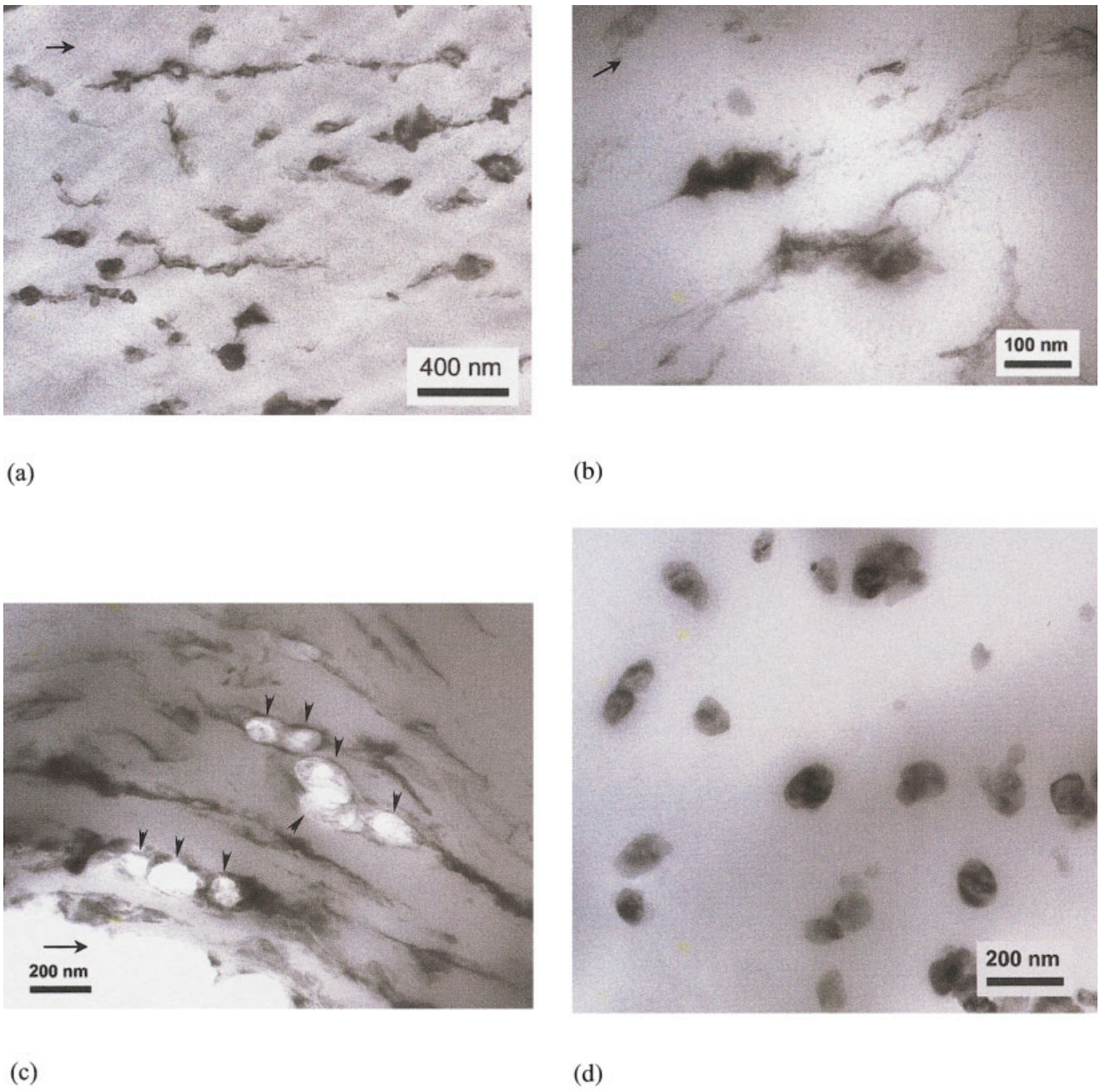

Figure 4 TEM of DN-4PB Charpy impact-tested PP/$CaCO_3$ specimen taken from (a) 120 μm above the crack surface, (b) 60 μm above the crack surface, (c) immediately above the crack surface, and (d) undamaged region. The arrow indicates the crack propagation direction. [Color figure can be viewed in the online issue, which is available at www.interscience.wiley.com.]

Study of fracture process, based on the DN-4PB Charpy impact specimens

The DN-4PB Charpy impact test was employed to investigate the detailed toughening mechanism in the PP/$CaCO_3$ nanocomposite. The DN-4PB technique is one of the most effective ways of generating a subcritical crack-tip damage zone.[23–25] The key toughening mechanism(s) and the sequence of toughening events can be unambiguously identified in the arrested crack-tip damage zone region, using a variety of microscopy techniques.

When OM is conducted, massive crazing (Fig. 3(a)) and birefringent plastic deformation (Fig. 3(b)) around the arrested crack tip are observed. The intensive plastic deformation is evidenced by the presence of a birefringent zone encapsulated by a larger light scattering cavitation zone, indicating that shear-yielding mechanism occurs along the crack wake. These dam-

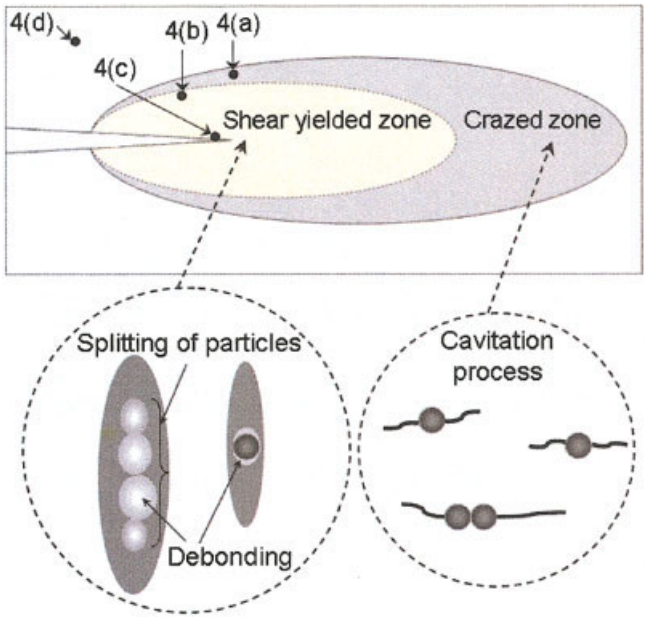

Figure 5 Schematic of the deformation mechanism in the DN-4PB Charpy impact-tested PP/$CaCO_3$ specimen. The regions of the TEM taken in Figure 4 are marked. [Color figure can be viewed in the online issue, which is available at www.interscience.wiley.com.]

age features are similar to the damage features observed in other toughened polymers,[23–27] suggesting that massive crazing is effective in facilitating plastic deformation of PP matrix. TEM study is further employed to confirm the aforementioned conjecture.

To learn about the early stages of the toughening process, it is necessary to investigate the damage feature far away from the crack tip, but inside the damage zone. TEM observation at about 120 μm above the crack-tip region has been made, and the presence of small, but widespread crazes was found (Fig. 4(a)). Interestingly, these crazes appear to be initiated by the $CaCO_3$ nanoparticles. This indicates that the $CaCO_3$ nanoparticles act as effective stress concentrators, which help trigger craze formation and growth. However, based on the TEM finding, it is unclear whether or not $CaCO_3$ nanoparticles have debonded from the PP matrix to allow for craze growth. It is possible that since the specimen being analyzed has been unloaded, any prior debonding process during loading would have been recovered from the snap-back of the PP matrix upon unloading, especially when the scale of plastic deformation is small, i.e., away from the crack-tip region.

In the region at the transition between the light-scattering craze zone and the birefringent shear-banding zone, the crazes appear to be more diffuse and slightly distorted (Fig. 4(b)). This finding is consistent with our earlier observation on the toughening mechanisms found in nylon 6,6/polyphenylene ether and PP/Noryl systems.[24,26] However, no sign of $CaCO_3$ nanoparticles debonding is observed in this region, either.

To check whether or not possible debonding of $CaCO_3$ nanoparticles from the PP matrix has taken place, TEM micrographs were taken immediately below the fracture surface near the crack tip (Fig. 4(c)). The crazes were further smeared by the shear-banding process, making the crazes even more defused and less well defined. Careful observation reveals that some of the $CaCO_3$ nanoparticles have debonded from the PP matrix (See arrows in Fig. 4(c)). This finding is consistent with the recent work of Chan et al., who have shown that $CaCO_3$ nanoparticles can be easily debonded from the PP matrix, upon tensile loading.[14] For reference, the morphology of the intact, undeformed PP/$CaCO_3$ is shown in Figure 4(d).

Figure 5 summarizes the operative toughening mechanisms found in PP/$CaCO_3$ nanocomposite, based on the aforementioned microscopy study. The $CaCO_3$ nanoparticles appear to be effective stress concentrators to help initiate and grow massive crazes. Therefore, the cavitational process, which is a prerequisite process for promoting shear-banding mechanism in the plane-strain region,[26–29] is triggered by massive crazing at the crack-tip region.

It should be noted that judging that the crazes are initiated near the equatorial region of the $CaCO_3$ nanoparticles or their small aggregates, particle-matrix debonding or splitting of aggregated nanoparticles should have taken place before the formation of crazes. This is simply because the maximum stress concentration site around an inclusion is located at the equatorial region, if the inclusion phase is softer than the matrix phase. Since the $CaCO_3$ nanoparticles are much harder than the PP matrix, the $CaCO_3$ nanoparticles should have been debonded or split between the aggregated particles before the crazes were initiated.

Study of fracture process, based on the Izod impact specimens

The incorporation of $CaCO_3$ in PP has significantly increased the Izod impact strength of the PP matrix (Table II). As shown in Figure 6, neat PP, under bright-field OM, exhibits brittle and featureless failure with-

TABLE II
Impact Strengths of the PP and PP/$CaCO_3$ Nanocomposites

Sample	Impact strength (J/m)
Neat PP	55.2 ± 2.0
PP/$CaCO_3$[a]	128.6 ± 9.9

[a] 9.2 vol % of $CaCO_3$ nanoparticle, with mixing time of 30 min.

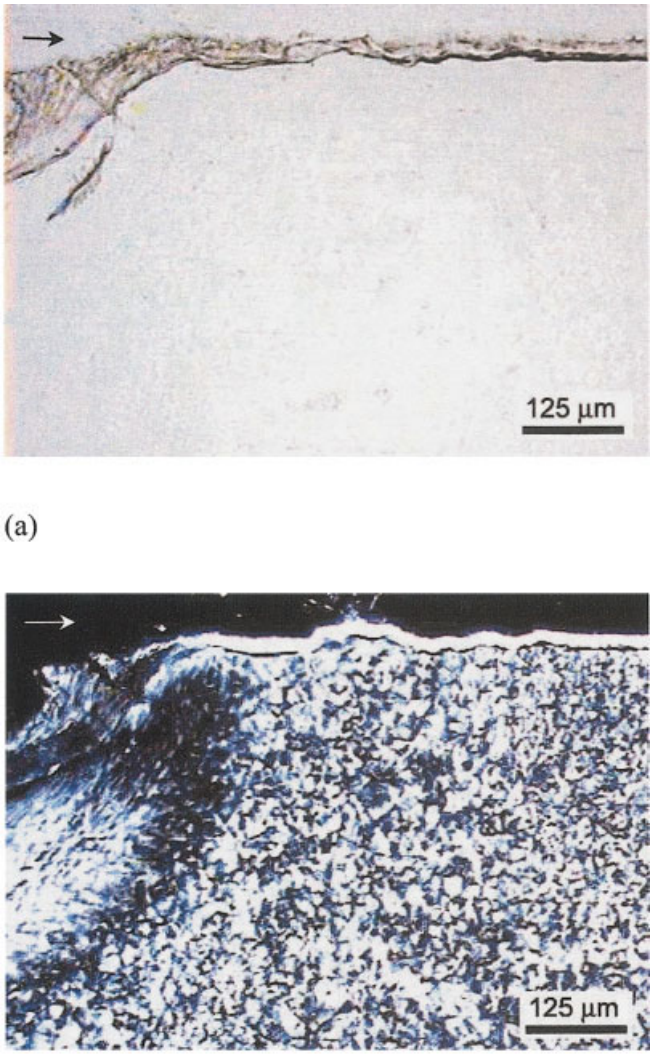

Figure 6 TOM of neat PP: (a) bright field and (b) cross polarized field. The arrow indicates the crack propagation direction. [Color figure can be viewed in the online issue, which is available at www.interscience.wiley.com.]

out any sign of significant plastic deformation. On the other hand, the PP/$CaCO_3$ nanocomposite exhibits extensive microcracking or crazing or both on the subsurface damage zone (Fig. 7). This behavior results in a higher impact strength for PP/$CaCO_3$ nanocomposite.

Unfortunately, the specimens after the Izod impact tests do not preserve the information regarding the sequence of toughening events upon impact fracture. The advancing crack during the impact test has obliterated the operative fracture mechanisms along the crack tip and crack wake. No useful information can be extracted from further microscopy investigation, using TEM. Comparison of results obtained between the DN-4PB Charpy impact tests and the Izod impact tests clearly indicates the usefulness of the DN-4PB Charpy impact tests for deciphering the impact toughening sequence of events of polymeric materials. Therefore, the DN-4PB impact test is recommended for identification and fundamental understanding of toughening mechanisms of polymers upon impact fracture.

The present study shows that debonding and splitting of the aggregated $CaCO_3$ nanoparticles, which lead to massive crazing in PP, have helped trigger crack-tip shear banding of PP matrix. The impact strength of PP is thus significantly improved. The present study also suggests that it is possible to use nanometer-sized rigid filler to toughen PP matrix and, in the meantime, increase the modulus of PP. Al-

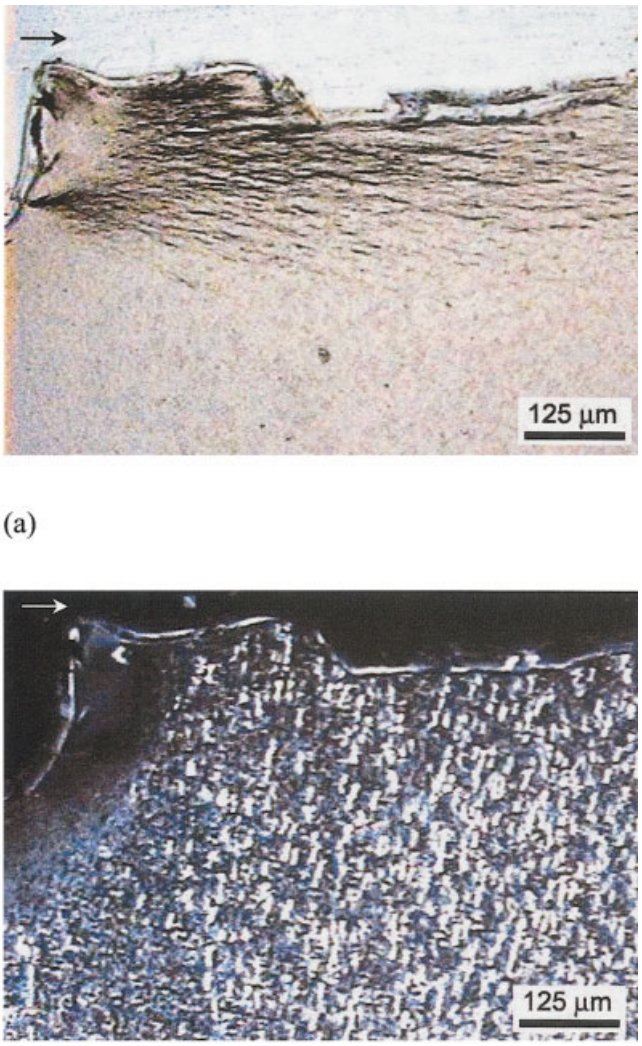

Figure 7 TOM of PP/$CaCO_3$ nanocomposite: (a) bright field and (b) cross polarized field. The arrow indicates the crack propagation direction. [Color figure can be viewed in the online issue, which is available at www.interscience.wiley.com.]

though the $CaCO_3$ nanoparticles do not appear to exhibit strong adhesion to PP matrix, the thermally induced contraction of PP against the $CaCO_3$ nanoparticles, upon cooling during molding of specimens, produces sufficiently strong interfacial adhesion to prevent premature debonding between PP and the $CaCO_3$ nanoparticles. Thus, $CaCO_3$ nanoparticles turn out to be effective for improving both modulus and impact strength of PP.

It is noted that $CaCO_3$ particles are quite effective in initiating crazes in this study (Fig. 4(a)). Even for particles as small as 40–50 nm in size, signs of craze formation around those small particles are still present. This finding is in direct contradiction to many of the rubber[28,29] and rigid polymer[26] toughened PP systems we have investigated in the past, where only particles of a size of 300 nm or higher would show effectiveness in initiating crazes. One possible explanation to account for the discrepancy is that the $CaCO_3$ particles have helped to nucleate the formation of β-phase PP around the $CaCO_3$ particles, making it much easier to trigger the formation of crazes. Another possibility is that, during loading, the voids formed by debonding from the $CaCO_3$ particles grow to a significant size, to allow for crazes to initiate and grow. The aforementioned conjectures, though plausible, still await further verification.

CONCLUSIONS

The morphology and impact toughening mechanisms in PP/$CaCO_3$ nanocomposite were investigated using OM and TEM techniques. It is clearly observed that the addition of $CaCO_3$ nanoparticles positively altered the spherulite size, crystal structure, and toughenability in PP matrix. In this study, the main toughening mechanisms of the PP/$CaCO_3$ nanocomposite are massive crazing, followed by shear banding of the matrix. This leads to impressive improvements in both impact strength and modulus of PP matrix.

References

1. Tyan, H.-L.; Liu, Y.-C.; Wei, K.-H. Chem Mater 1999, 11, 1942.
2. Hasegawa, N.; Okamoto, H.; Kawasumi, M.; Usuki, A. J Appl Polym Sci 1999, 74, 3359.
3. Gam, K. T.; Miyamoto, M.; Nishimura, R.; Sue, H.-J. Polym Eng Sci 2003, 43, 1635.
4. Sue, H.-J.; Gam, K. T.; Bestaoui, N.; Spurr, N.; Clearfield, A. Chem Mater 2004, 16, 242.
5. Pinnavaia, T. J.; Lan, T.; Kaviratna, P. D.; Wang, M. S. Mater Res Soc Symp Proc 1994, 346, 81.
6. Lan, T.; Pinnavaia, T. J. Chem Mater 1994, 6, 2216.
7. Messersmith, P. B.; Giannelis, E. P. J Polym Sci: Part A: Polym Chem 1995, 33, 1047.
8. Hasegawa, N.; Kawasumi, M.; Kato, M.; Usuki, A.; Okada, A. J Appl Polym Sci 1998, 67, 87.
9. Kawasumi, M.; Hasegawa, N.; Kato, M.; Usuki, A.; Okada, A. Macromolecules 1997, 30, 6333.
10. Kurokawa, Y.; Yasuda, H.; Kashiwagi, M.; Oyo, A. J Mater Sci Lett 1997, 16, 1670.
11. Usuki, A.; Kato, M.; Okada, A.; Kurauchi, T. J Appl Polym Sci 1997, 63, 137.
12. Kato, M.; Usuki, A.; Okada, A. J Appl Polym Sci 1997, 66, 1781.
13. Kurokawa, Y.; Yasuda, H.; Oya, A. J Mater Sci Lett 1996, 15, 1481.
14. Chan, C.-M.; Wu, J.; Li, J.-X.; Cheung, Y.-K. Polymer 2002, 43, 2981.
15. Hoffmann, H.; Grellmann, W.; Zilvar, V. Polymer Composites, Walter de Gruyter: New York, 1986.
16. Badran, B. M.; Galeski, A.; Kryszewski, M. J Appl Polym Sci 1982, 27, 3669.
17. Liu, Z. H.; Kwok, K. W.; Li, R. K. Y.; Choy, C. L. Polymer 2002, 43, 2501.
18. Thio, Y. S.; Argon, A. S.; Cohen, R. E.; Weinberg, M. Polymer 2002, 43, 3661.
19. Holik, A. S.; Kambour, R. P.; Hobbs, S. Y.; Fink, D. G. Microstruct Sci 1979, 7, 357.
20. Friedrich, K. Adv Polym Sci 1983, 52/53, 225.
21. Ouederni, M.; Philips, P. J. J Engng Appl Sci 1996, 2, 2312.
22. Labour, T.; Ferry, L.; Gauthier, C.; Hajji, P.; Vigier, G. J Appl Polym Sci 1999, 74, 195.
23. Sue, H.-J.; Yee, A. F. J Mater Sci 1993, 28, 2915.
24. Sue, H.-J.; Yee, A. F. J Mater Sci 1989, 24, 1447.
25. Sue, H.-J. Polym Eng Sci 1991, 31, 270.
26. Wei, G.-X.; Sue, H.-J.; Chu, J.; Huang, C.; Gong, K. J Mater Sci 2000, 35, 555.
27. Sue, H.-J. J Mater Sci 1992, 27, 3098.
28. Wei, G.-X.; Sue, H.-J. Polym Eng Sci 2000, 40, 1979.
29. Li, Y.; Wei, G.-X.; Sue, H.-J. J Mater Sci 2002, 37, 2447.